Journal of Zhejiang University SCIENCE A
ISSN 1673-565X (Print); ISSN 1862-1775 (Online)
www.zju.edu.cn/jzus; www.springerlink.com
E-mail: jzus@zju.edu.cn

An approach for shape optimization of stratosphere airships based on multidisciplinary design optimization*

Quan-bao WANG†, Ji-an CHEN, Gong-yi FU, Deng-ping DUAN

(*Institute of Aerospace Science & Technology, Shanghai Jiao Tong University, Shanghai 200240, China*)

†E-mail: quanbaowang@sjtu.edu.cn

Received Nov. 21, 2008; Revision accepted Apr. 20, 2009; Crosschecked Sept. 10, 2009

Abstract: Airship shape is crucial to the design of stratosphere airships. In this paper, multidisciplinary design optimization (MDO) technology is introduced into the design of airship shape. We devise a composite objective function, based on this technology, which takes account of various factors which influence airship performance, including aerodynamics, structures, energy and weight to determine the optimal airship shape. A shape generation algorithm is proposed and appropriate mathematical models are constructed. Simulation results show that the optimized shape gives an improvement in the value of the composite objective function compared with a reference shape.

Key words: Airship shape, Multidisciplinary design optimization (MDO), Adaptive simulation annealing, Stratosphere airship
doi:10.1631/jzus.A0820814 **Document code:** A **CLC number:** V27

INTRODUCTION

Stratosphere airships have been attracting increasing attention for decades, for aerial exploration, environmental monitoring, and surveillance purposes (Colozza and Dolce, 2005). An airship is a lighter-than-air vehicle which produces significant lift resulting from buoyancy. The airship body, which generates the lift, plays an important role in airship design. The shape of an airship directly influences its aerodynamic and structural characteristics. The payload, maximum operating altitude, endurance and location are determined by the body volume. The aerodynamic drag, surface area of the envelope and area of the solar array are determined by the shape. Aerodynamic considerations are reflected in the minimum drag coefficient, structural considerations affect the minimum surface area, minimum solar battery area and hoop stress, and energy considerations influence the solar area, all of which have a direct affect on envelope weight. Thus, it is essential to investigate shape optimization in airship design.

Generally, the design of airship shape has depended mainly on the experience of the designer. Some designers have chosen existing shapes without optimizing the shape in the design process (Ozoroski *et al*., 2003; Pant, 2003). Others have optimized the shape in consideration only of aerodynamic characteristics and have ignored other factors (Lutz and Wagner, 1998; Nejati and Matsuuchi, 2003; Wang and Shan, 2006).

In this paper, multidisciplinary design optimization (MDO) technology is introduced into the design of airship envelope shape for the purpose of obtaining the optimum shape in relation to a number of factors. A shape generation algorithm in accordance with MDO is proposed. The factors, including aerodynamics, structure, energy and weight, are analyzed and appropriate mathematical models are constructed. A composite objective function reflecting the multidisciplinary nature of the problem is devised and the shape optimization of an airship is performed using an adaptive simulation annealing algorithm.

* Project (No. 2007AA705003) supported by the National Hi-Tech Research and Development Program (863) of China

NATURE OF MULTIDISCIPLINARY ASPECTS

Aerodynamics, structures, energy and weight directly influence the design of airships, each having their own constraints and demands. From the perspective of aerodynamics, it is especially important to find a drag-minimized envelope (i.e., with a minimum volumetric drag coefficient) during the shape design of an airship. From a structural perspective, the shape design needs to reduce the hoop stress and from an energy perspective, airship shape is designed with the purpose of minimizing the surface area of the solar array while satisfying the energy requirements of the airship. Using the empirical expressions given by Khoury and Gillett (1999), an increase in fineness ratio can be shown to reduce the drag and resulting fuel load, but induce an increase in hoop stress, which causes higher structural bending moments and structural weight. This shows just one of the possible interactions among various factors. It leads to the conclusion that, from the viewpoint of MDO, shape optimization needs to take account of all possible interactions among different variables and find the optimum shape of the airship which satisfies the specifications and requirements posed by diverse factors that directly affect airship performance.

SHAPE GENERATION ALGORITHM

To explore the possibility of designing better shapes using multidisciplinary optimization characteristics, a new shape generation algorithm is proposed to extend the range of design space. The equation of the airship body is denoted as

$$64(y^2+z^2)=a(l-x)(bx-l\sqrt{c}+\sqrt{cl^2-dlx}), \quad (1)$$

where x, y and z are x-, y- and z-coordinate of points on airship curve, respectively, l is the length of the envelope and a, b, c and d are the shape parameters of the airship.

The characteristics of optimal shapes obtained are compared with a reference shape (Fig.1).

Since the complete airship body is obtained by revolving the 2D shape by 360° about the x-axis, the 2D shape equation can be transformed as follows:

$$y=\sqrt{a(l-x)(bx-l\sqrt{c}+\sqrt{cl^2-dlx})}/8. \quad (2)$$

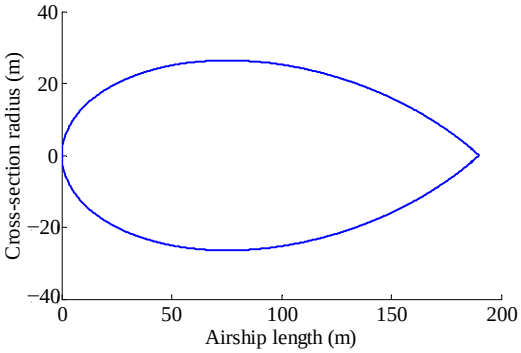

Fig.1 Reference shape

MODELS OF DISCIPLINES DESCRIPTION

To minimize aerodynamic drag, weight and structural requirements and to maximize energy generated by the solar array in the envelope design, the objectives of shape optimization are to minimize the volumetric drag coefficient, the surface area, hoop stress and the surface area of the solar array. Since high fidelity analysis is very time-consuming, low fidelity models from the literature have been integrated into the present optimizer to perform the optimization.

Model of volumetric drag coefficient

The volumetric coefficient of drag (C_{DV}), which is calculated based on $V^{2/3}$, was given by Khoury and Gillett (1999) as a function of fineness ratio (l/D) and is described as follows:

$$C_{DV}=\frac{0.172(l/D)^{1/3}+0.252(D/l)^{1.2}+1.032(D/l)^{2.7}}{Re^{1/6}}, \quad (3)$$

$$Re=\frac{\rho_a vl}{\mu}, \quad (4)$$

where D is the maximum diameter of the envelope, Re is Reynolds number, v is the velocity of wind, ρ_a is the density of air and μ is the dynamic viscosity of air.

Model of surface area

The surface area of the envelope can be calculated as follows:

$$A_e = 2\pi\int_0^a y\left(1+\left(\frac{dy}{dx}\right)^2\right)^{0.5} dx. \quad (5)$$

Model of minimum hoop stress

The minimum hoop stress per unit thickness is obtained using Eq.(6). The minimum inner pressure (ΔP) in Eq.(6) consisting of static pressure (p_{static}), Munk pressure (p_{dyn}) and internal differential pressure (p_{diff}) is shown in Eq.(7). Static pressure caused by static bending moments, Munk pressure caused by the dynamic bending moments and internal differential pressure are calculated using Eq.(8), Eq.(9) and Eq.(10), respectively.

$$\sigma_{min} = \Delta PD/2, \quad (6)$$

$$\Delta P = p_{static} + p_{dyn} + p_{diff}, \quad (7)$$

$$p_{static} = 2.263\rho_a r_{gc}\lambda^2, \quad (8)$$

$$p_{dyn} = \rho_a v^2 V_e(k_2 - k_1)(\sin 2\alpha)/(\pi r_{gc}^3), \quad (9)$$

$$p_{diff} = 1.722 g\rho_a R\lambda \sin\alpha, \quad (10)$$

where g is the acceleration because of gravity, r_{gc} is the radius of the envelope at the mass center, $\lambda=l/D$ is the fineness ratio, k_1 and k_2 are the Munk inertial factors of longitudinal and transverse directions, respectively, α is the angle of attack, and R is the maximum radius.

Model of surface area of solar array

The power required to run an airship and its payloads consists mostly of control systems (p_{ctrls}), payload systems (p_{pays}) and propulsion systems (p_{props}). Of these, the propulsion systems use by far the greatest amount of energy. Around 100 kW of propulsion power is required when flying at 25 m/s. The payload systems use around 10 kW and the control system about 11 kW (Natio *et al.*, 1999), both of which can be assumed to be constant during design. The total power required can be described as follows:

$$p_{total} = p_{pays} + p_{ctrls} + p_{props}. \quad (11)$$

The energy used for propulsion can be calculated as

$$p_{props} = F_{prop} v/\eta_{prop}, \quad (12)$$

$$F_{prop} = \rho_a v^2 C_{DV} V_e^{2/3}/2, \quad (13)$$

$$V_e = \pi\int_0^l y^2 dx, \quad (14)$$

where v is the speed of the airship, η_{prop} is the efficiency of the propulsion systems, l is the length of the airship, and V_e is the volume of the envelope.

The total energy is denoted as

$$Q_{total} = k_{energy} p_{total} t, \quad (15)$$

where k_{energy} is the factor of energy and t is the time in days.

For the purpose of calculating the area of the solar array, the shape of the airship can be assumed to approximate a cylinder. The radius of the envelope at the mass center (r_{gc}) is adopted as the radius of the cylinder. Thus, a vector which defines any point on the surface can be created as a function of the radius of a cylinder (r_{gc}), location (x) and angle along the circumference (γ), and is given by

$$\boldsymbol{P}(x,y,z) = (x, r_{gc}\sin\gamma, r_{gc}\cos\gamma). \quad (16)$$

Using Eq.(16), the normal vector of the surface is

$$\bar{\boldsymbol{n}}(x,y,z) = (0, \sin\gamma, \cos\gamma). \quad (17)$$

The sun elevation angle (β) and the azimuth angle (α) are changing with time, changing the direction of the solar incidence ray (Fig.2). The normal vector of solar radiation is

$$\bar{\boldsymbol{l}}_{sunO} = \begin{pmatrix} \sin\alpha\cos\beta \\ \cos\alpha\cos\beta \\ \sin\beta \end{pmatrix}. \quad (18)$$

The solar radiation vector can be resolved into two parts: one perpendicular to the solar array surface and one parallel to it. Of these two parts, only the perpendicular part of the solar radiation vector is effective in producing electrical energy. This perpendicular part can be calculated using the dot product of the solar vector and the local normal vector of the

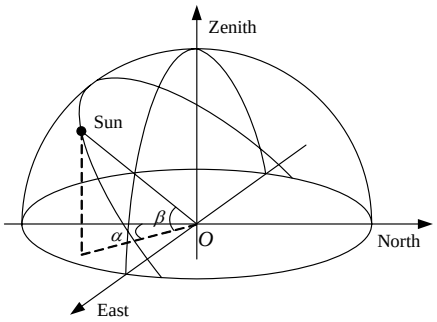

Fig.2 Sketch of sun angles

solar array surface, providing that these two vectors are relative to the same axis system. For this purpose, the solar radiation vector is transformed to the local airship axis system using Eq.(19):

$$\bar{\boldsymbol{l}}_{\text{sun}} = \boldsymbol{T}_{\text{m}} \cdot \bar{\boldsymbol{l}}_{\text{sunO}} = \boldsymbol{T}_{\text{m}} \cdot \begin{pmatrix} \sin\alpha\cos\beta \\ \cos\alpha\cos\beta \\ \sin\beta \end{pmatrix}, \tag{19}$$

where $\boldsymbol{T}_{\text{m}}$ is a transformation matrix, which transforms the vector from the universal axis system to the local airship axis system. The contents of this matrix depend on the attitude and direction of the airship, and are expressed as Eq.(20) and shown at the bottom of this page, where Θ is the airship pitch angle, Φ is the airship roll angle and Ψ is the airship yaw angle (0° for east, 270° for north).

When an airship is flying eastwards without any pitch and roll (Θ=0, Φ=0, Ψ=0), the matrix becomes

$$\boldsymbol{T}_{\text{m}} = \begin{pmatrix} 1 & 0 & 0 \\ 0 & 1 & 0 \\ 0 & 0 & 1 \end{pmatrix}. \tag{21}$$

Thus, the solar radiation perpendicular to the surface (I_{b}) can be obtained from

$$I_{\text{b}} = I_{\text{n}} \frac{\bar{\boldsymbol{n}} \cdot \bar{\boldsymbol{l}}_{\text{sun}}}{|\bar{\boldsymbol{n}}| \cdot |\bar{\boldsymbol{l}}_{\text{sun}}|}, \tag{22}$$

where I_{n} is the intensity of the sunlight.

The amount of electrical energy generated from an area ds can be calculated as

$$\text{d}W = I_{\text{b}} \cdot \eta_{\text{solar}} \text{d}s, \tag{23}$$

where ds is the product of the length along the x-direction and the length along the circumference

$$\text{d}s = \text{d}x \cdot r_{\text{gc}} \text{d}\gamma. \tag{24}$$

The total amount of energy received on the solar array is

$$Q_{\text{sun}} = \int_x \int_\gamma \int_t I_{\text{n}} \frac{\bar{\boldsymbol{n}} \cdot \bar{\boldsymbol{l}}_{\text{sun}}}{|\bar{\boldsymbol{n}}| \cdot |\bar{\boldsymbol{l}}_{\text{sun}}|} \eta_{\text{solar}} r_{\text{gc}} \text{d}t\text{d}\gamma\text{d}x. \tag{25}$$

For the airship to work normally, the energy should satisfy

$$Q_{\text{sun}} = Q_{\text{total}}. \tag{26}$$

The surface area of the solar array can be obtained easily using Eqs.(15), (25) and (26) with numerical method, and is described as

$$A_{\text{sa}} = \int_x \int_\gamma r_{\text{gc}} \text{d}\gamma\text{d}x. \tag{27}$$

SHAPE OPTIMIZATION OF AIRSHIP

Design vector

There are four shape coefficients in Eq.(1), namely a, b, c, d. To investigate the effect of relaxing the length constraint, the length is kept in the design vector. Thus, the design vector of the concerned problem is described as $\boldsymbol{X}_{\text{D}} = (a, b, c, d, l)$.

Constraints

The volume of the airship is fixed for the comparability of the design results. The range of the

$$\boldsymbol{T}_{\text{m}} = \begin{pmatrix} \cos\Theta\cos\Psi & \cos\Theta\sin\Psi & -\sin\Theta \\ -\cos\Phi\sin\Psi + \sin\Phi\sin\Theta\cos\Psi & \cos\Phi\cos\Psi + \sin\Phi\sin\Theta\sin\Psi & \sin\Phi\cos\Theta \\ \sin\Phi\sin\Psi + \cos\Phi\sin\Theta\cos\Psi & -\sin\Phi\cos\Psi + \cos\Phi\sin\Theta\sin\Psi & \cos\Phi\cos\Theta \end{pmatrix}, \tag{20}$$

length is set taking into account the shape and length of airships in general. The constraints are shown as $V = 2.5\times10^5\ \mathrm{m}^3, 160\ \mathrm{m} \le l \le 200\ \mathrm{m}$.

Objective function

To consider the influences of various factors on the optimization of shape, a composite objective function involving C_{DV}, A_{e}, $\sigma_{\min}$, and A_{sa} is devised as follows:

$$F_{\mathrm{composite}} = \frac{1}{4}\times\left(\frac{C_{\mathrm{DV}}}{C_{\mathrm{DVF}}}+\frac{A_{\mathrm{e}}}{A_{\mathrm{eF}}}+\frac{\sigma_{\min}}{\sigma_{\mathrm{minF}}}+\frac{A_{\mathrm{sa}}}{A_{\mathrm{saF}}}\right)\times100, \tag{28}$$

where C_{DVF}, A_{eF}, σ_{minF}, and A_{saF} are the respective initiation values of C_{DV}, A_{e}, $\sigma_{\min}$, and A_{sa} corresponding to the reference shape.

Other objective functions adopted for comparison with the composite function described above are as follows:

$$F_{\mathrm{o1}} = \frac{C_{\mathrm{DV}}}{C_{\mathrm{DVF}}}\times100, \tag{29}$$

$$F_{\mathrm{o2}} = \frac{\sigma_{\min}}{\sigma_{\mathrm{minF}}}\times100. \tag{30}$$

ADAPTIVE SIMULATION ANNEALING ALGORITHM

Adaptive simulated annealing (ASA) is employed to perform the shape optimization. ASA (Ingber, 1993) is a variant of simulated annealing (SA). SA is a random-search technique which exploits an analogy between the way in which a metal cools and freezes into a minimum energy crystalline structure (the annealing process) and the search for a minimum in a more general system.

To force some material into a low energy state, we heat it and make it reach a high temperature T_0 by imparting high energy to it. Then we cool it slowly, allowing it to come to thermal equilibrium at each temperature. This strategy of a controlled decrease in temperature leads to a crystallized solid state, which is stable and corresponds to a minimum of energy. The physical process described above was associated with combinatorial optimization problems (Kirkpatrick *et al*., 1983). An objective function is associated with the energy of a physical system and system dynamics are imitated by random local modifications of the current solution. In SA, the annealing process is simulated at several such temperature steps by letting the system reach equilibrium at each temperature. To simulate how the system reaches thermodynamic equilibrium at each fixed temperature in the schedule of decreasing temperatures, the Metropolis algorithm (Metropolis *et al*., 1953) is employed. Thus, the SA algorithm not only accepts changes that decrease the objective function (assuming a minimization problem), but also some changes that increase it, which makes it avoid being trapped in local minima. In the SA algorithm, key parameters are the initial temperature, the annealing schedule which mandates how the temperature is decremented, and the number of iterations at each step (Banerjee and Dutt, 2004).

Compared to standard SA algorithms, ASA employs a new annealing schedule for each temperature as

$$T(k) = T_0\exp(-ck^{1/N}), \tag{31}$$

where $T(k)$ is the temperature of the annealing schedule in annealing-time steps k, T_0 is the starting temperature and is large enough, c is a constant and N is the number of parameters.

The annealing schedule is faster than fast Cauchy annealing (Szu and Hartley, 1987), where $T=T_0/k$, and much faster than Boltzmann annealing (Kirkpatrick *et al*., 1983), where $T=T_0/\ln k$. ASA algorithm is well suited to solving high non-linear problems with short running codes, when finding the global optimum is more important than a quick improvement in the design (Ingber, 1993), and so suits very well the optimization problem described above.

To ensure that the optimizer performs efficiently, some control parameters in ASA (Table 1) had to be adjusted to suit the objective function. Inappropriate parameter settings can make the algorithm extremely inefficient and may even result in failure to arrive at the global optimum.

The values of ‘Max. number of generated designs’ and ‘Convergence epsilon’ are determined by numerical experimentation while the values of other

parameters are those recommended by Ingber (1993) based on previous experience. A higher penalty is forced on the objective function for an undesirable shape resulting from the shape generation algorithm.

Table 1 Control parameters of ASA

Control parameter	Value
Max. number of generated designs	10 000
Convergence epsilon	1×10^{-3}
Number of designs for convergence check	5
Relative rate of parameter annealing	1.0
Relative rate of cost annealing	1.0
Relative rate of parameter quenching	1.0
Relative rate of cost quenching	1.0
Max. number of failed designs	5

RESULTS AND DISCUSSION

In this section, we describe the results from performing optimization using an adaptive SA algorithm to resolve the problem described above.

Firstly, we optimized the shape using objective function F_{o1}. Fig.3 shows the optimized shape in comparison with the reference shape. Comparisons with respect to C_{DV}, A_e, σ_{min}, A_{sa} and objective function F_{o1} are shown in Table 2. Little improvement was gained in terms of C_{DV} or A_{sa}. The reason is that the design of the reference shape focused on the lowest volumetric coefficient of drag C_{DV} under the given operating conditions. Thus, it had an objective function similar to that of the optimization above, giving little improvement in C_{DV}.

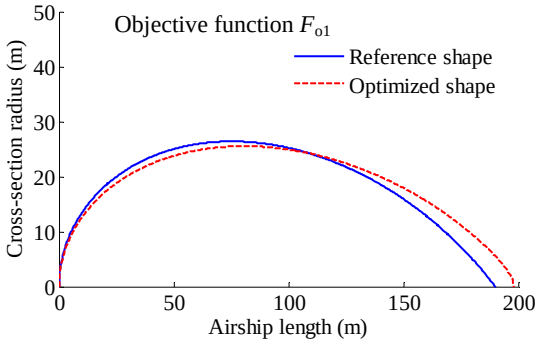

Fig.3 Comparison between the shape optimized with F_{o1} and the reference shape

A similar optimization was carried out with objective function F_{o2}. The shape obtained was compared to the reference shape (Fig.4). The comparison in terms of C_{DV}, A_e, σ_{min}, A_{sa} and F_{o2} is shown in Table 3. From Fig.4 we conclude that the shape generation algorithm prefers to have a minimum airship length for minimum hoop stress.

Table 2 Results from comparisons between the reference shape and the optimized shape (F_{o1})

	Reference shape	Optimized shape	Improvement (%)
C_{DV}	0.02397	0.02370	1.13
A_e	23644.6	24249.7	−2.56
σ_{min}	6044.1	6293.3	−4.12
A_{sa}	10182.2	10070.9	1.09
F_{o1}	100.00	98.87	1.13

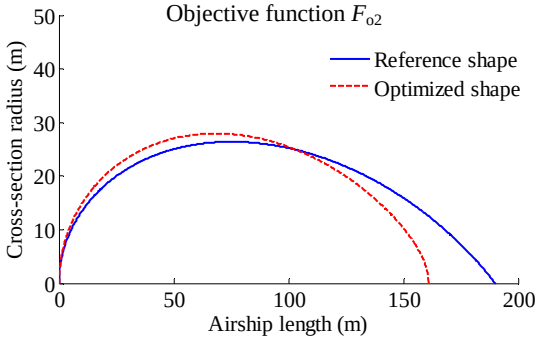

Fig.4 Comparison between the shape optimized with F_{o2} and the reference shape

Table 3 Results from comparisons between the reference shape and the optimized shape (F_{o2})

	Reference shape	Optimized shape	Improvement (%)
C_{DV}	0.02397	0.02565	−7.01
A_e	23644.6	22429.6	5.14
σ_{min}	6044.1	5093.2	15.73
A_{sa}	10182.2	10870.1	−6.76
F_{o1}	100.00	84.27	15.73

So far, the optimizations described were carried out using only a single objective function. To appreciate the multidisciplinary aspect of optimization, the composite objective function described as Eq.(28) was incorporated into the optimizer. The comparison between the optimized shape and the reference shape

is shown in Fig.5. The numerical values of four objective functions compared with the reference shape are presented in Table 4. The results show that the optimal shape has a 2.10% improvement in the value of the composite objective function compared with the reference shape.

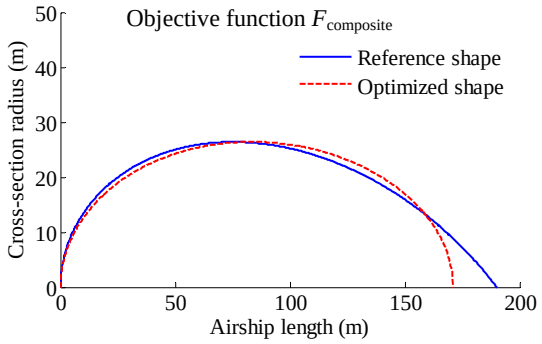

Fig.5 Comparison between the shape optimized with the composite objective function and the reference shape

Table 4 Results from comparisons between the reference shape and the optimized shape ($F_{composite}$)

	Reference shape	Optimized shape	Improvement (%)
C_{DV}	0.02397	0.02460	−2.63
A_e	23644.6	23117.7	2.23
σ_{min}	6044.1	5368.9	11.17
A_{sa}	10182.2	10425.9	−2.39
F_{o1}	100.00	97.90	2.10

To demonstrate more clearly the advantages of an MDO approach to this problem, the optimized shapes corresponding to the objective functions F_{o1} and F_{o2} in terms of $F_{composite}$ were calculated using Eq.(28). Comparisons with respect to $F_{composite}$ between the reference shape and the optimized shape using different objective functions are shown in Table 5.

Table 5 Comparisons between the reference shape and the shapes optimized with different objective functions

	$F_{composite}$	Improvement (%)
Reference shape	100.00	
Optimized shape F_{o1}	101.12	−1.12
Optimized shape F_{o2}	98.23	1.77
Optimized shape $F_{composite}$	97.90	2.10

The results show that the composite objective function value with the objective function $F_{composite}$ turns out to be lower than the objective functions F_{o1} and F_{o2}.

CONCLUSION

In the process of designing stratosphere airships, some designers do not consider optimization of the airship shape while others optimize the shape using an objective function related to only a single factor. In this paper, MDO is introduced into the shape design of airships for considering the influence of various factors and obtaining the best shape. A shape generation algorithm is proposed and models of each factor are constructed. A composite objective function is devised based on the optimum targets of minimum drag, minimum surface, minimum hoop stress and minimum surface of solar array. An adaptive SA algorithm is adopted for the optimization, and the result of simulations show the validity of this method.

References

Banerjee, S., Dutt, N., 2004. Very Fast Simulated Annealing for HW-SW Partitioning. Technical Report CECS-TR-04-17, University of California, Irvine.

Colozza, A., Dolce, J.L., 2005. High-altitude, Long-endurance Airships for Coastal Surveillance. NASAPTM-2005-213427.

Ingber, L., 1993. Adaptive Simulated Annealing (ASA), Global Optimization C-code. Caltech Alumni Association, Pasadena, California. Available from: http://www.ingber.com/#ASA−CODE [Accessed 13/09/08; verified 01/02/09].

Khoury, G.A., Gillett, J.D., 1999. Airship Technology. Cambridge University Press, Cambridge.

Kirkpatrick, S., Gelatt, C.D.Jr., Vecchi, M.P., 1983. Optimization by simulated annealing. *Science*, **220**(4598):671- 680. [doi:10.1126/science.220.4598.671]

Lutz, T., Wagner, S., 1998. Drag reduction and shape optimization of airship bodies. *Journal of Aircraft*, **35**(3):345-351.

Metropolis, N., Rosenbluth, A., Rosenbluth, M., Teller, A., Teller, E., 1953. Equation of state calculations by fast computing machines. *Journal of Chemical Physics*, **21**(6):1087-1092.

Natio, H., Eguchi, K., Hoshino, T., Okaya, S., Fujiwara, T., Miwa, S., Nomura, Y., 1999. Design Concept and Analysis of Solar Power Subsystem for SPF Airship Operation. AIAA 99-3913.

Nejati, V., Matsuuchi, K., 2003. Aerodynamics design and genetic algorithms for optimization of airship bodies. *JSME International Journal, Series B: Fluids and Thermal Engineering*, **46**(4):610-617. [doi:10.1299/jsmeb.46.610]

Ozoroski, T.A., Mas, K.G., Hahn, A.S., 2003. A PC-based Design and Analysis System for Lighter-than-air Unmanned Vehicles. 2nd AIAA "Unmanned Unlimited" System, Technologies, and Operation-Aerospace, San Diego, California, USA.

Pant, R.S., 2003. A Methodology for Determination of Baseline Specifications of a Non-rigid Airship. AIAA's 3rd Annual Aviation Technology, Integration, and Operation (ATIO) Technical Forum, Denver, Colorado, USA.

Szu, H., Hartley, R., 1987. Fast simulated annealing. *Physics Letters A*, **122**(3/4):157-162. [doi:10.1016/0375-9601(87)90796-1]

Wang, X.L., Shan, X.X., 2006. Shape optimization of stratosphere airship. *Journal of Aircraft*, **43**(1):283-287.